

A New Solid-State Zinc–Air Battery for Fast Charge

Siyuan Zhao, Kelian Wang,* Shuxian Tang, Xiaotian Liu, Kelin Peng, Yu Xiao, and Yu Chen

Rechargeable zinc–air batteries (ZAB) with solid-state electrolyte are a potential power source for flexible electronic devices. However, solid electrolytes for the battery at large currents remain a challenge in bubble removal at the electrode surface and the small contact area of the electrolyte–electrode interface, as well as low conductivity itself. Herein, a three-electrode structure is proposed for the solid-state rechargeable ZAB, where the sodium polyacrylate (PAA-Na) hydrogel serving as the electrolyte exhibits good mechanical properties, excellent water retention ability, and high conductivity (0.19 S cm^{-1}) after being soaked in potassium hydroxide and zinc acetate solution. The zinc electrode of porous structure is sandwiched by the electrolyte on both sides, facilitating ion transport during charge/discharge. MnO_2/C , as the catalyst of the air electrode, is in contact with the hydrogel, increasing the catalyst active area. Nickel mesh is the charging electrode which facilitates the removal of the evolved bubbles. The results demonstrate that rechargeable ZAB with the PAA-Na hydrogel electrolyte can release a maximum power density of 100.7 mW cm^{-2} and run for 183 cycles at a current density of 10 mA cm^{-2} , which can be a strong competitor in the flexible energy-storage field.

1. Introduction

With the rapid development of flexible electronic devices, traditional cumbersome batteries are no longer suitable for their power sources.^[1,2] Therefore, it is of great imperativeness to develop next-generation batteries with reliability and flexibility.^[3–6] Compared with traditional commercial lithium-ion batteries (LIBs), zinc–air batteries (ZABs) are superior in terms of energy density, safety, and cost, which are expected to become ideal substitutes for LIBs.^[7–10] However, conventional ZABs with aqueous electrolyte suffer from electrolyte leakage and dendrite growth.^[11,12] In addition, sometimes it even requires a bulky pump to circulate the electrolyte, which is not possible in simple and lightweight power sources.^[13] In contrast, most solid-state ZABs for flexible

energy-storage devices are not capable of fast charging because of the limitation of bifunctional catalysts and accumulation of oxygen bubbles generated during charging.


Currently, two main types of solid electrolytes are suitable for flexible ZABs.^[14] One is to insert hydroxyl functional groups into the polymer membrane backbone, where the thinness of membrane ensures flexibility while hydroxide ions ensure battery operation.^[15,16] The other one is to use a water-absorbent gel electrolyte which can obtain moisture and hydroxide ions by immersing it in an alkali solution.^[17,18] Under the condition of the same flexibility, the ionic conductivity of the second electrolyte is usually larger than that of the first electrolyte, and the synthesis step of the second is relatively simple as well. Therefore, the gel electrolyte is more suitable for rechargeable ZABs in certain aspects. Polyvinyl alcohol (PVA) is a common material used for gel electrolytes,

which are usually made into a single phase with good mechanical properties and ductility.^[19,20] However, PVA has a poor water absorption capacity and alkali resistance, resulting in low ionic conductivity, which severely limits the cycling performance of solid-state batteries. Subsequently, polyacrylic acid (PAA) and polyacrylamide (PAM), which have better alkali-absorbing abilities than PVA, were used as the gel electrolyte of rechargeable ZABs.^[21,22] Although PAA and PAM can provide higher conductivity than PVA, these two gels generally have poor mechanical properties in the case of saturated water absorption, especially when absorbing salt solutions. For this purpose, Alam et al. reviewed the function of carbon nanomaterials like graphene oxide (GO) in enhancing the mechanical strength of polymer hydrogel.^[23] Nevertheless, these fillers are usually expensive and cannot be applied to inexpensive large-scale production. Therefore, the research focus lies in obtaining a high water absorption performance while also ensuring the low cost and good mechanical properties of the hydrogel.

Bifunctional electrodes are widely used in rechargeable ZABs.^[13,24] However, when charging the solid-state ZABs at high current densities ($\approx 10 \text{ mA cm}^{-2}$), a large number of oxygen bubbles will evolve rapidly and accumulate but cannot escape in time, which will impede electrolyte–electrode contact and invalidate the air electrode. Moreover, as a potential solution, the traditional three-electrode structure, namely, two different electrodes, respectively, works as the charging and discharging electrode, and the zinc electrode that is located between the

S. Zhao, Dr. K. Wang, X. Liu, Y. Xiao
School of Mechanical Engineering
Beijing Institute of Technology
Beijing 100081, China
E-mail: wangkl@bit.edu.cn

S. Tang, K. Peng, Y. Chen
School of Materials Science and Engineering
Beijing Institute of Technology
Beijing 100081, China

 The ORCID identification number(s) for the author(s) of this article can be found under <https://doi.org/10.1002/ente.201901229>.

DOI: 10.1002/ente.201901229

two electrodes is also not suitable for solid-state ZABs because the zinc ions continuously consumed during charging cannot be replenished by the discharging process due to blocking of the zinc plate.

To solve the challenges of ionic transport and fast charging, here, we develop a rechargeable solid-state ZAB with a sodium polyacrylate (PAA-Na) hydrogel electrolyte and an improved three-electrode structure. The self-standing PAA-Na hydrogel can be freely compressed, stretched, and twisted and can ensure good mechanical properties even after absorbing salt solution. In addition, rich PAA-Na long chains render the hydrogel good water absorption and retention ability, accommodate more hydroxide ions, and achieve high ionic conductivity. In contrast, on the basis of the traditional three-electrode structure, the improved three-electrode structure breaks the barrier of the zinc plate using a type of porous zinc to make the two sides of the electrolyte come into close contact, thereby ensuring the replenishment of zinc ions in the charging side through the free movement of zinc ions between two sides. In addition, we found that the retaining three-electrode structure, which facilitates oxygen bubbles' removal through nickel the mesh and ensures the stability of the charge/discharge cycle, is more suitable for solid-state ZABs when charging at a large current density.

2. Results and Discussion

2.1. Structure Characteristics of the PAA-Na Hydrogel

The transparent PAA-Na hydrogel is synthesized through solution polymerization of acrylic acid (AA) neutralized by NaOH using ammonium persulfate (APS) as the initiator and *N,N'*-methylenebis (acrylamide) (BIS) as the cross-linker, as shown in **Figure 1a**. To prove the successful synthesis of PAA-Na hydrogel, Fourier-transform infrared spectroscopy

(FT-IR) was conducted. As shown in **Figure 1b**, the peaks emerging at 1548, 1406, and 1114 cm^{-1} show the formation of acrylates (1548 and 1406 cm^{-1} for COO^- , and 1114 cm^{-1} for C—O in ester). PAA-Na is a unique material for its excellent water and ion absorption ability, in which a porous structure provides enough space to reserve water and facilitate ion transport (Figure 1c). Due to the electrostatic repulsion between the ions on chains, the polymer chains stretch, causing osmotic pressure inside and outside the network structure. Then water molecules diffuse into the network structure in an infiltration manner to form PAA-Na hydrogel.^[25] At the same time, the interconnected network structure and hydrogen bonds of the hydrogel itself limit the infinite expansion and ensure the overall fastening of the hydrogel. So, the PAA-Na hydrogel was immersed in a concentrated solution of 6 M potassium hydroxide (KOH) and 0.2 M zinc acetate ($\text{Zn}(\text{CH}_3\text{COO})_2$) for sufficient time to make it an excellent electrolyte for rechargeable ZAB, as water and concentrated ions in the hydrogel provide enough access for ion transport.

2.2. Hydrophilic and Conductive Properties of the PAA-Na Hydrogel

Liquid electrolyte uptake ability is of great importance for the ionic conductivity of hydrogel, as water is the carrier of ion transport. To better illustrate the super absorbency of PAA-Na hydrogel, it was compared with another hydrogel PAM which was widely used in rechargeable ZABs. By soaking the fully dried hydrogels in the solution of 6 M KOH and 0.2 M $\text{Zn}(\text{CH}_3\text{COO})_2$, the curves of electrolyte absorption ratio over time were obtained. The ratio increases with time and becomes stable after 24 h, as shown in **Figure 2a**, meaning that hydrogel reaches a state of equilibrium. It is worth noting that the final electrolyte uptake ratio of PAA-Na reaches 1370%, which is three times that of PAM. Moreover, PAA-Na hydrogel has a faster rate of water

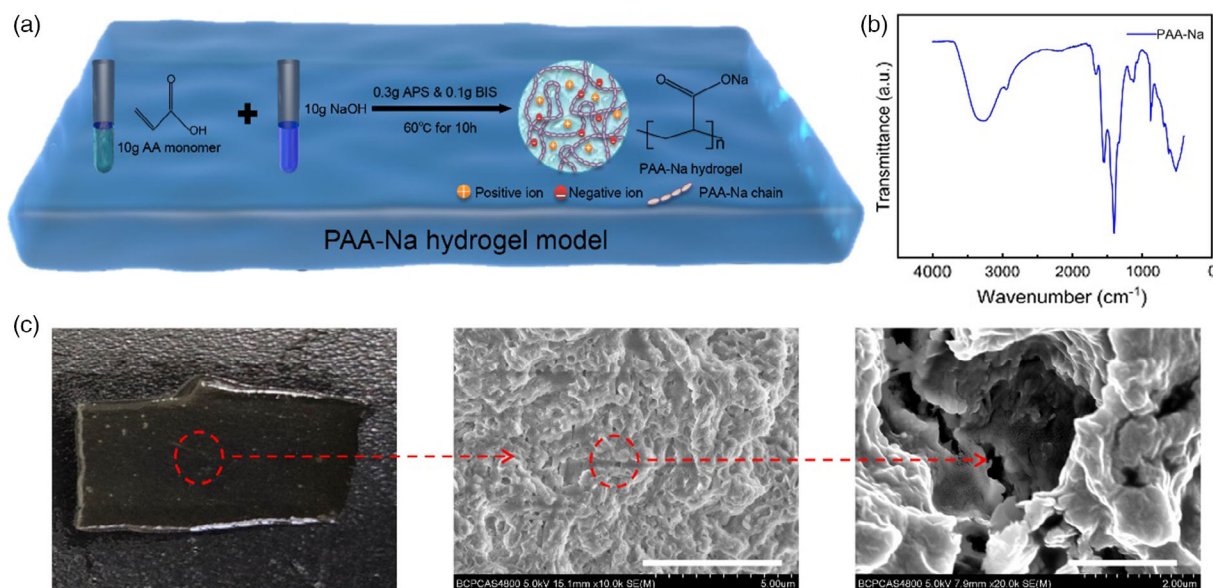


Figure 1. a) Schematic diagram of synthesis process of the PAA-Na hydrogel, b) FT-IR spectra of PAA-Na hydrogel, c) optical photo of real PAA-Na hydrogel (length: 3.5 cm, width: 1.5 cm), and the SEM images of its porous microstructure. Scale bar: 5 and 2 μm , respectively.

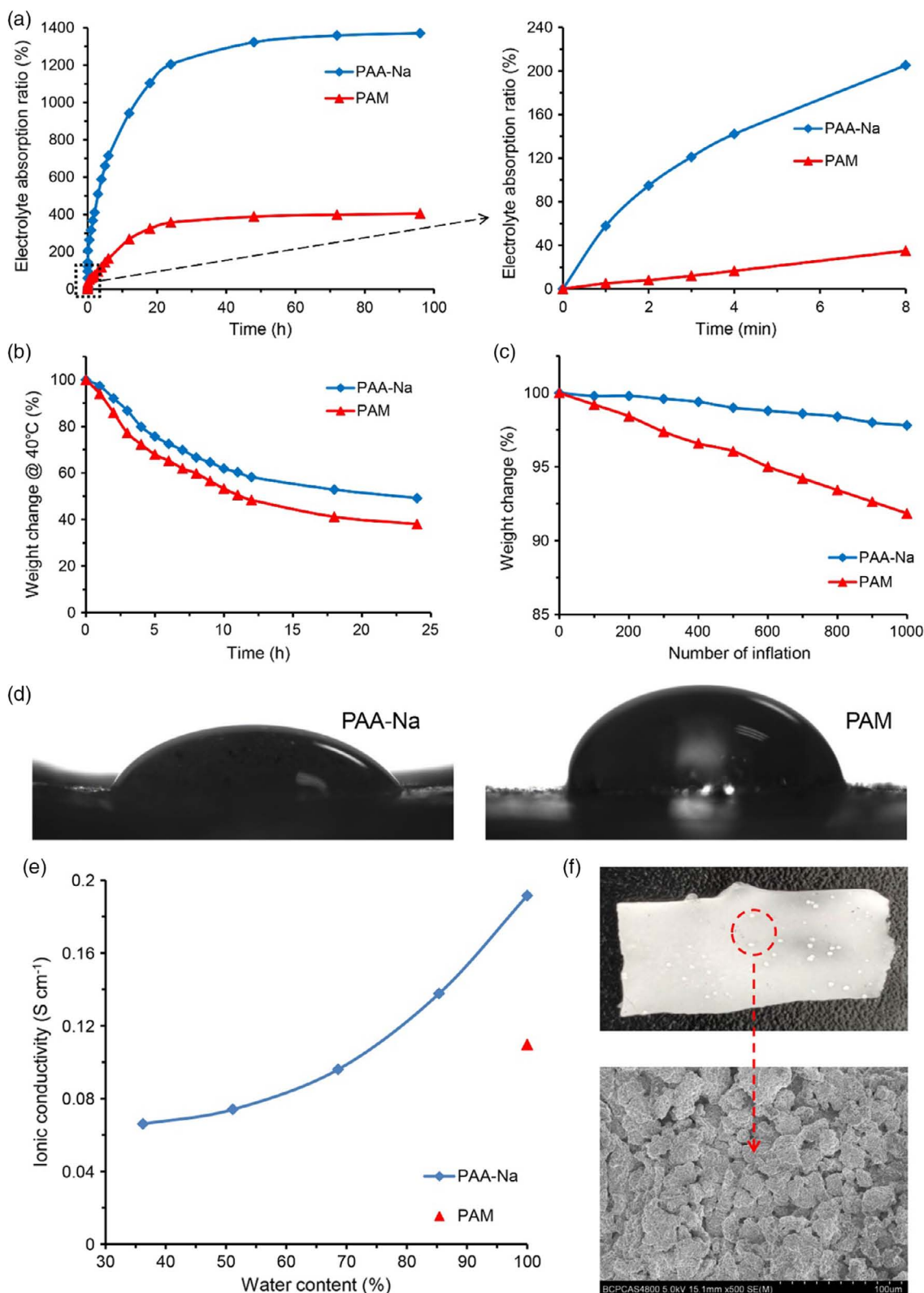


Figure 2. a) Liquid electrolyte uptake ability of PAA-Na and PAM hydrogels, b) water retention ability of PAA-Na and PAM hydrogel at 40 °C oven, c) water retention ability of PAA-Na and PAM hydrogel after inflation, d) contact angle of PAA-Na and PAM hydrogel, e) ionic conductivity of PAA-Na hydrogel under different water contents and fully saturated PAM hydrogel, and f) photograph of hydrogel after water loss and SEM image of hydrogel after complete drying.

absorption than PAM hydrogel. In just 1 min, the PAA-Na hydrogel absorbed 60% of its own weight of electrolyte, whereas the PAM hydrogel absorbed only 35% of its own weight of electrolyte in 8 min.

Equally significantly, PAA-Na hydrogel also exhibits the brilliant liquid electrolyte retention ability that is the basis for long-term stable cycles of rechargeable ZAB. In consideration of battery heating and hydrogel electrolytes in high-temperature situations, the electrolyte retention capacity of hydrogels was tested at 40 °C. Figure 2b shows that the PAA-Na hydrogel can still maintain an electrolyte above 50% of its maximum content after 24 h compared with the PAM hydrogel. In addition, oxygen bubbles generated during charging will take away part of water, inflating the hydrogel simulated in Figure 2c (about 1900 cm³ air per inflation) and demonstrating that PAA-Na hydrogel lost electrolyte only 2.2% of its maximum content after 1000 times inflation behavior, significantly less than that of PAM hydrogel. The carboxyl groups in the PAA-Na chains have a better hydrophilic activity than the amide groups in the PAM chains. Although PAM is hydrolyzed in alkaline solution where amino groups are replaced by oxygen in hydroxyl groups, the reaction is not complete and finally leaves a polymer hydrogel with both acrylamide and acrylate terminal groups. In addition, the PAA-Na hydrogel has a smaller contact angle than PAM hydrogel, as shown in Figure 2d, which also verifies that PAA-Na has a better electrolyte uptake and retention ability than PAM and carboxyl groups that have a better hydrophilic activity than amino groups. Finally, the aforementioned scanning electron microscope (SEM) images of dried PAA-Na reveal a pore-rich network entangled by hydrophilic PAA-Na chains, guaranteeing interspace for sufficient liquid electrolyte.

The ionic conductivity of hydrogel electrolyte plays an essential role in the battery performance such as operating voltage and cycle number, whereas the absorbed hydroxide ions (OH⁻) contribute the most to ionic conductivity.^[26] In particular, OH⁻ is also the key ion in the reaction of ZAB. So, the alkali-resistant PAA-Na hydrogel electrolyte with the property of accommodating and retaining more OH⁻ becomes a strong competitor. With more OH⁻ and water available inside the polymer network of hydrogel electrolyte, a higher ionic conductivity is a natural result. As PAA-Na hydrogel can absorb the liquid electrolyte three times than that of PAM hydrogel, the saturated PAA-Na hydrogel reaches the ionic conductivity of 0.19 S cm⁻¹, which is almost twice that of saturated PAM hydrogel (Figure 2e), even two to three orders of magnitude higher than that of most conventional polymer electrolytes.^[27–29] In contrast, as water facilitates the movement of free OH⁻, lack of water will seriously affect the ionic conductivity of hydrogel electrolyte. As expected, the ionic conductivity decreases with the decrease in water content. Even more, when the water content of the electrolyte is too low (i.e., 30%), KOH and zinc hydroxide (Zn(OH)₂) particles^[30] are precipitated in a large amount (Figure 2f), blocking the path of ion transport, which leads to a much lower ionic conductivity than when fully saturated. Therefore, the PAA-Na hydrogel electrolyte with excellent electrolyte retention ability can always maintain a high level of ionic conductivity and ensure long-term stable operation of the ZAB.

2.3. Mechanical Property of the PAA-Na Hydrogel

Polymer hydrogel electrolytes with good mechanical properties coupled with bendable electrodes can endow practical and commercial utility to flexible energy-storage devices. From the tensile stress–strain curves of PAA-Na and PAM hydrogel, PAA-Na hydrogel shows a better mechanical property than PAM hydrogel. In addition, the PAA-Na hydrogel can be stretched, folded, rolled, twisted, and crumpled without any crack and damage, as shown in Figure 3b, exhibiting good flexibility. This observation is due to the stress exerted to the hydrogel being dispersed onto entangled PAA-Na chains which distribute uniformly in the hydrogel. However, under higher water content, the mechanical properties of the hydrogel will decrease significantly for the decreased density of PAA-Na polymer chains in unit volume.^[31] In consideration of the volume of the three-electrode structure, the compressibility of PAA-Na hydrogel containing saturated liquid electrolyte was tested. In Figure 3c, the PAA-Na hydrogel can be compressed to 60% of its original thickness without any mechanical failure, ensuring its potential practical use in flexible energy-storage devices.

2.4. Rechargeable Three-Electrode ZAB with PAA-Na Hydrogel

The electrochemical impedance spectroscopy (EIS) measurement on rechargeable ZAB in Figure 4a shows that the battery with PAA-Na hydrogel electrolyte has a smaller diameter of the semicircle in the Nyquist plot, meaning a low charge transfer resistance. In addition, the resistance of PAA-Na is smaller than that of PAM hydrogel due to the better ability of water uptake. Figure 4b shows the polarization and power density curves of hydrogel-based batteries. Impressively, the open-circuit voltage of ZAB using PAA-Na hydrogel is 1.37 V, whereas the battery with PAM is 1.28 V. ZAB with PAA-Na hydrogel can still reach 0.74 V at the current density of 135.1 mA cm⁻², whereas for PAM electrolyte, the same discharging voltage of the battery is obtained at the current density of 91.48 mA cm⁻². Moreover, the peak power density of the PAA-Na-based battery reaches 100.7 mW cm⁻² because of the higher ionic conductivity of PAA-Na hydrogel electrolyte and better contact between the air electrode and PAA-Na hydrogel electrolyte, much higher than that of PAM-based battery (67.9 mW cm⁻²). From the rate performance shown in Figure 4c, ZABs with PAA-Na hydrogel electrolyte have a stable and high voltage plateau over continuous operations of different current densities. To verify the battery's practical use in discharging, two ZABs packaged by aluminum films were connected in series to illuminate a 2.5 V light bulb (Figure 4c).

The use of a three-electrode structure is a simple and inexpensive choice to fast charge the hydrogel-based ZAB. However, all-solid ZABs with the three-electrode configuration have two problems. One is that zinc ions in the charging side cannot be replenished, the other is that oxygen bubbles generated during charging cannot escape in time. To solve the problem of ion transport, a type of porous zinc plate was used, ensuring the close contact of hydrogels on both sides of the zinc electrode. In addition, nickel mesh was also used to allow oxygen bubbles escape easily. As shown in Figure 4d, zinc plate is sandwiched in the

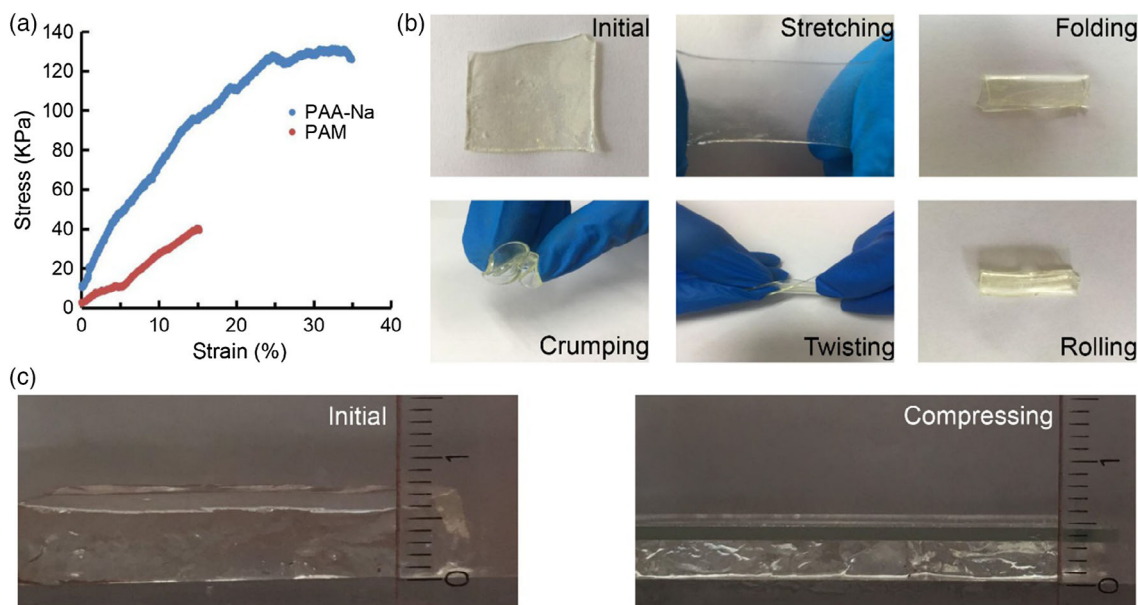


Figure 3. a) Stress–strain curves of PAA-Na and PAM hydrogels, b) photographs of mechanical deformation of the PAA-Na hydrogel, and c) photographs of initial and 60% compressed PAA-Na hydrogel.

middle of two hydrogel electrolytes, where the air electrode and charging electrode are closely attached to them, respectively. In the optimization of the three-electrode structure, the battery with the support of PAA-Na hydrogel electrolyte exhibits a stable performance at high current density (10 mA cm^{-2} , 12 min per cycle). Figure 4e shows that the PAA-Na-based ZAB using a three-electrode structure exhibits a stable initial discharge voltage of 1.13 V and a charge voltage of 1.98 V, which is superior to that of PAM-based battery (1.06 and 2.04 V). In addition, the PAA-Na-based battery has a stable charge–discharge cycle, whereas the charging voltage of the PAM-based battery increases rapidly to 2.2 V after 18 cycles. The result proves that PAA-Na hydrogel is more suitable as a solid electrolyte for ZABs, demonstrating that the three-electrode structure can be used for solid-state batteries as well.

A compact three-electrode structure was reported in our previous works, which is combining nickel mesh and air electrode together like bifunctional catalysts (structure 2, the aforesaid structure called structure 1).^[32] To verify the feasibility of this structure in hydrogel-based batteries, the cycling performance of rechargeable ZAB was tested. As shown in Figure 4f, the battery with structure 2 quickly reaches the charge voltage of 2 V due to the more complete contact between PAA-Na hydrogel electrolyte and nickel mesh. However, when charging at 10 mA cm^{-2} , a large amount of oxygen bubbles is generated rapidly and have nowhere to escape. With the accumulation of bubbles, the charging voltage gradually increases to 2.5 V. At the same time, oxygen bubbles not only deactivate the catalyst and oxidize activated carbon in the air electrode, but also block the contact between hydrogel electrolyte and air electrode, resulting in the loss of discharging ability. In contrast, as the charging electrode and the air electrode were, respectively, located on both sides of zinc in structure 1, the discharging process was not interfered by

charging. Moreover, when the battery was discharged, bubbles generated by the large current density charging had enough time to escape from the mesh of the nickel net, ensuring cycle stability.

To further demonstrate the cycling performance of PAA-Na-based three-electrode ZAB, galvanostatic charge and discharge (GCD) measurements at the large current density (10 mA cm^{-2} , 12 min per cycle) were carried out (Figure 4g), where the battery can run for 183 cycles before the charging voltage reaches 2.5 V and the discharging voltage only drops by 0.09 V (from 1.13 to 1.04 V) and the charging voltage just increases by 0.13 V (from 1.98 to 2.11 V) after 100 cycles. The cycling performance of the battery is highly dependent on the use of a three-electrode structure and PAA-Na hydrogel electrolyte. Moreover, the newly introduced nickel mesh avoids the accumulation of oxygen bubbles and damage to the air electrode, endowing good discharging performance in GCD. At the same time, PAA-Na hydrogel electrolyte with superior water absorption and retention ability provides the basis for long-term cycling, as well as high ionic conductivity for battery reaction.

3. Conclusions

We first proposed the three-electrode structure applied to the solid-state rechargeable ZAB for improving the battery lifetime at a large current density. Meanwhile, PAA-Na hydrogel synthesized through monomer polymerization and cross-linking achieved a superior ionic conductivity (0.19 S cm^{-1}) and mechanical property as well as liquid electrolyte absorption and retention ability. As a result, the PAA-Na based three-electrode ZAB exhibited a superior electrochemical performance with a maximum power density of 100.7 mW cm^{-2} and 183 cycles at a current

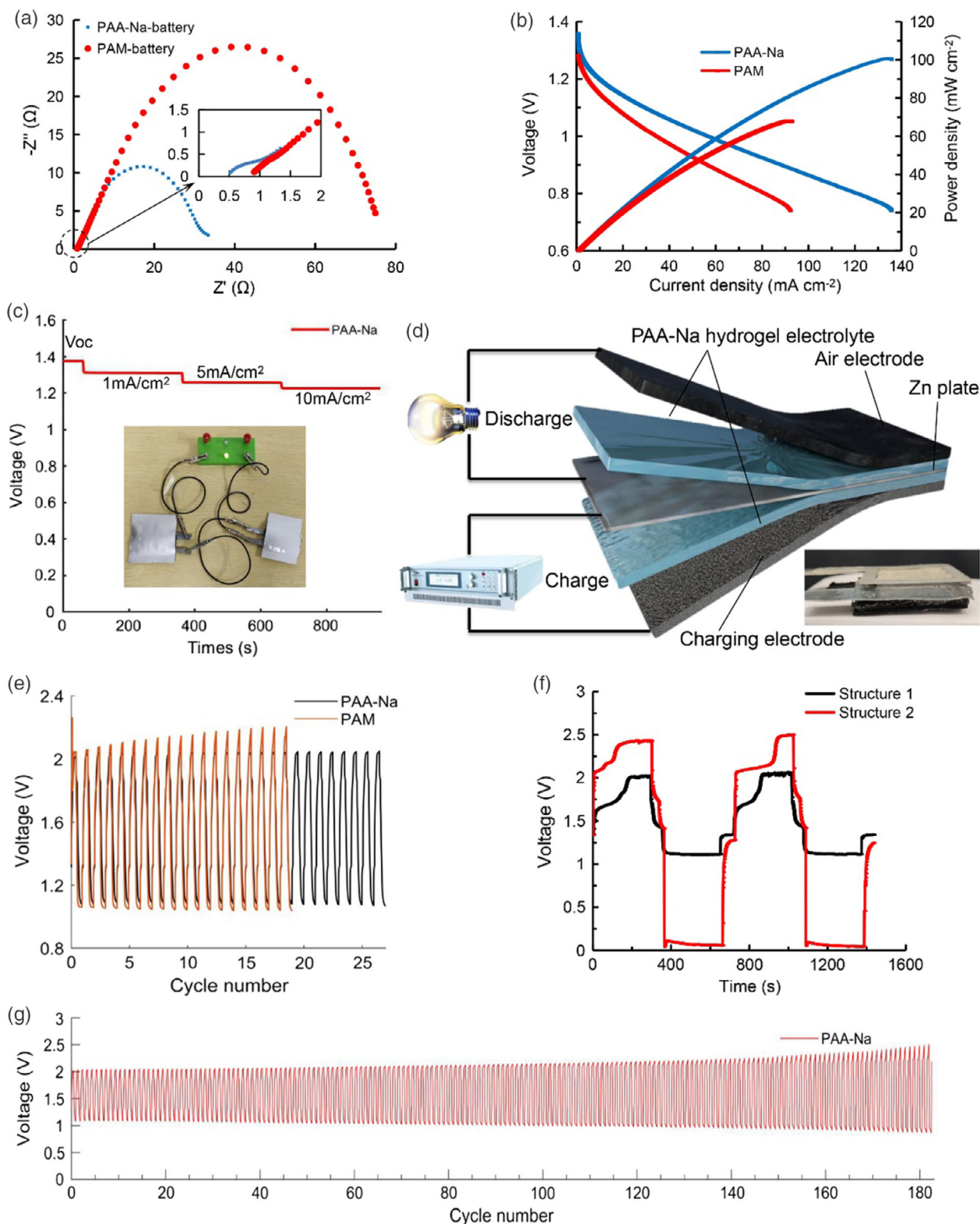


Figure 4. a) Impedance tests of PAA-Na- and PAM-based ZAB, b) LSV (1 mV s^{-1}) and power density curves of PAA-Na- and PAM-based ZAB, c) discharge curves at different current densities of 0, 1, 5, and 10 mA cm^{-2} , inner picture shows two PAA-Na-based ZABs connected in series to illuminate a 2.5 V light bulb, d) schematic diagram and optical photo of the three-electrode ZAB, e) cycling performance of PAA-Na- and PAM-based ZAB at a current density of 10 mA cm^{-2} , f) cycling performance of PAA-Na-based ZAB with different structures at a current density of 10 mA cm^{-2} , and g) cycling performance of PAA-Na-based ZAB with the three-electrode structure at the current density of 10 mA cm^{-2} .

density of 10 mA cm^{-2} , demonstrating that the feasibility of the three-electrode structure will be in application of the solid-state rechargeable ZABs in the field of fast charge.

4. Experimental Section

All chemicals used in the synthesis of PAA-Na and PAM were purchased from Aladdin. Nickel net and zinc electrode (thickness of 0.08 mm) and air electrode were bought from Changsha Spring Energy Corporation.

Synthesis of PAA-Na: PAA-Na hydrogel was synthesized via initiating polymerization of a mixed solution of AA and sodium hydroxide (NaOH) using APS as the initiator and BIS as the cross-linker. First, 10 g NaOH was dissolved in 20 mL deionized (DI) water, and 10 mL AA monomers were added into 20 mL DI water. Then, NaOH solution was slowly dropped into the AA solution within 1 h under stirring to obtain a mixed solution. Before polymerization, the solution was degassed with nitrogen for 20 min to remove the dissolved particles. After that, 0.3 g APS and 0.1 g BIS were added into the mixed solution and stirred for 30 min in the ice water bath. Subsequently, the polymerization and vacuum drying process were conducted in a 60°C oven for 10 h. Finally, the fully dried PAA-Na film was soaked into 6 M KOH and 0.2 M ZnO solution to obtain the PAA-Na hydrogel electrolyte for rechargeable ZABs.

Synthesis of PAM: The synthesis of PAM followed a well-established method. First, 2 g acrylamide was dissolved in 5 mL distilled water. Then, 5 mg BIS as cross-linker and 8 mg APS as initiator were added into the aforementioned solution and maintained at 40°C for 30 min under stirring. Before polymerization, the solution was degassed with nitrogen for 20 min to remove the dissolved particles. After that, free-radical polymerization was conducted at 60°C for 30 min.

Characterization and Electrochemical Detection: The water retention test of PAA-Na and PAM hydrogels was conducted in an 40°C vacuum drying oven, and the water taken away by oxygen test was conducted by an inflator in the ambient environment. The contact angle test was conducted by an optical contact angle measuring instrument (Zhijia Equipment, Shenzhen, China). A SEM (HITACHI, S-4800) was used to observe the cross-section and surface morphologies of freeze-drying PAA-Na hydrogel. PAA-Na electrolyte was placed between two stainless steel sheets, for measuring ionic conductivity from alternating current (AC) impedance spectra. Linear sweep voltammetry (LSV) curves were obtained under a scanning rate of 1 mV s^{-1} . EIS was measured in the frequency range of 0.01–10000 Hz with a magnitude of 10 mV (at open-circuit voltage). All the electrochemical tests mentioned earlier were conducted in an electrochemical workstation (CHI660E).

Assembly and Testing of Rechargeable ZAB: Rechargeable ZAB with the three-electrode structure was composed of zinc electrode, hydrogel electrolyte, air electrode, and the charging electrode, where zinc electrode was sandwiched tightly by hydrogel electrolytes on both sides, and air electrode as well as charging electrode were pressed upon the electrolyte, respectively. PAA-Na hydrogel after fully absorbing KOH and $\text{Zn}(\text{CH}_3\text{COO})_2$ solution was ready for the electrolyte. The loose and porous structure was used as the zinc electrode for smooth transmission of zinc ions, inexpensive manganese dioxide served as the catalyst of air electrode, and nickel mesh worked as the charging electrode, smoothly exhausting oxygen bubbles out of the battery during charge. The active reaction area of the electrodes was $40 \text{ mm} \times 50 \text{ mm}$. The GCD measurements and cycle tests on the prepared rechargeable ZAB were carried out by a battery testing system (Neware, CT-4004).

Acknowledgements

This work was supported by National Natural Science Foundation of China (21706013). The team acknowledges Analysis & Testing Center, Beijing Institute of Technology, for providing material characterizations.

Conflict of Interest

The authors declare no conflict of interest.

Author Contributions

S.Z. designed experiments and wrote the article. K.W. served as lead for the project and modified the article. S.T. helped with the synthesis of hydrogel. K.P. and Y.C. gave advice to the analysis of hydrogel structure. Y.X. and X.L. conducted the battery testing.

Keywords

large currents, rechargeable zinc–air batteries, sodium polyacrylate hydrogel, three electrode structures

Received: October 16, 2019

Revised: December 7, 2019

Published online: January 28, 2020

- [1] K. Tang, C. Yuan, Y. Xiong, H. Hu, M. Wu, *Appl. Catal. B Environ.* **260**, 118209.
- [2] S. Qu, Z. Song, J. Liu, Y. Li, Y. Kou, C. Ma, X. Han, Y. Deng, N. Zhao, W. Hu, C. Zhong, *Nano Energy* **2017**, 39, 101.
- [3] X. Wang, X. Lu, B. Liu, Y. T. Di Chen, G. Shen, *Adv. Mater.* **2014**, 26, 4763.
- [4] P. Tan, B. Chen, H. Xu, H. Zhang, W. Cai, M. Ni, M. Liu, Z. Shao, *Energy Environ. Sci.* **2017**, 10, 2056.
- [5] Z. Cao, H. Hu, M. Wu, K. Tang, T. Jiang, *J. Mater. Chem. A* **2019**, 7, 17581.
- [6] X. Chen, C. Zhong, B. Liu, Z. Liu, X. Bi, N. Zhao, X. Han, Y. Deng, J. Lu, W. Hu, *Small* **2018**, 14, 1702987.
- [7] J. M. Tarascon, M. Armand, *Nature* **2001**, 414, 359.
- [8] J.-S. Lee, S. Tai Kim, R. Cao, N.-S. Choi, M. Liu, K. T. Lee, J. Cho, *Adv. Energy Mater.* **2011**, 1, 34.
- [9] Y. Li, H. Dai, *Chem. Soc. Rev.* **2014**, 43, 5257.
- [10] K. Wang, P. Pei, Y. Wang, C. Liao, W. Wang, S. Huang, *Appl. Energy* **2018**, 225, 848.
- [11] K. Wang, Y. Xiao, P. Pei, X. Liu, Y. Wang, *J. Electrochem. Soc.* **2019**, 166, D389.
- [12] C.-Y. Chen, K. Matsumoto, K. Kubota, R. Hagiwara, Q. Xu, *Adv. Energy Mater.* **2019**, 9, 1900196.
- [13] H.-F. Wang, Q. Xu, *Matter* **2019**, 1, 565.
- [14] Y. J. Wang, J. Qiao, R. Baker, J. Zhang, *Chem. Soc. Rev.* **2013**, 42, 5768.
- [15] J. Zhang, J. Fu, X. Song, G. Jiang, H. Zarrin, P. Xu, K. Li, A. Yu, Z. Chen, *Adv. Energy Mater.* **2016**, 6, 1600476.
- [16] M. Wang, N. Xu, J. Fu, Y. Liu, J. Qiao, *J. Mater. Chem. A* **2019**, 7, 11257.
- [17] Z. Wang, H. Li, Z. Tang, Z. Liu, Z. Ruan, L. Ma, Q. Yang, D. Wang, C. Zhi, *Adv. Funct. Mater.* **2018**, 28, 1804560.
- [18] L. Ma, S. Chen, D. Wang, Q. Yang, F. Mo, G. Liang, N. Li, H. Zhang, J. A. Zapfen, C. Zhi, *Adv. Energy Mater.* **2019**, 9, 1803046.
- [19] C. C. Yang, S. J. Lin, *J. Power Sources* **2002**, 112, 497.
- [20] J. Fu, D. U. Lee, F. M. Hassan, L. Yang, Z. Bai, M. G. Park, Z. Chen, *Adv. Mater.* **2015**, 27, 5617.
- [21] Q. Liu, Z. Chang, Z. Li, X. Zhang, *Small Methods* **2018**, 2, 1700231.
- [22] M. J. Tan, B. Li, P. Chee, X. Ge, Z. Liu, Y. Zong, X. J. Loh, *J. Power Sources* **2018**, 400, 566.
- [23] A. Alam, Y. Zhang, H. C. Kuan, S.-H. Lee, J. Ma, *Progr. Polym. Sci.* **2018**, 77, 1.

- [24] X. Han, X. Ling, Y. Wang, T. Ma, C. Zhong, W. Hu, Y. Deng, *Angew. Chem.* **2019**, *131*, 5413.
- [25] M. Liu, T. Guo, *J. Appl. Polym. Sci.* **2001**, *82*, 1515.
- [26] Z. Pei, Y. Huang, Z. Tang, L. Ma, Z. Liu, Q. Xue, Z. Wang, H. Li, Y. Chen, C. Zhi, *Energy Storage Mater.* **2019**, *20*, 234.
- [27] J. Park, M. Park, G. Nam, J.-S. Lee, J. Cho, *Adv. Mater.* **2015**, *27*, 1396.
- [28] J. Fu, F. M. Hassan, J. Li, D. U. Lee, A. R. Ghannoum, G. Lui, Md. A. Hoque, Z. Chen, *Adv. Mater.* **2016**, *28*, 6421.
- [29] N. Vassal, E. Salmon, J. F. Fauvarque, *Electrochim. Acta* **2000**, *45*, 1527.
- [30] Y. Huang, Z. Li, Z. Pei, Z. Liu, H. Li, M. Zhu, J. Fan, Q. Dai, M. Zhang, L. Dai, C. Zhi, *Adv. Energy Mater.* **2018**, *8*, 1802288.
- [31] J. Liu, M. Hu, J. Wang, N. Nie, Y. Wang, Y. Wang, J. Zhang, Y. Huang, *Nano Energy* **2019**, *58*, 338.
- [32] K. Wang, C. Liao, W. Wang, Y. Xiao, X. Liu, S. Zhao, *Mater. Today Energy* **2019**, *14*, 100340.